$(NH_4)_6MnMo_9O_{32}$ AS OXYDESULFURIZATION CATALYST

M.G. EGUSQUIZA[†*], J. ACOSTA[†], M. MUÑOZ[†], G.P. ROMANELLI[†],
D. GAZZOLI[‡] and C.I. CABELLO[†§].

† *Centro de Investigación y Desarrollo en Cs. Aplicadas, Dr. J. J. Ronco. CINDECA, CCT-CONICET La Plata - CIC
- UNLP, Calle 47 N° 257, 1900, La Plata, Bs. As., Argentina.*
‡ *Dipartimento di Chimica, Sapienza Università di Roma, Ple. Aldo Moro 5, I-00185 Roma, Italia.*
§ *Facultad de Ingeniería-Universidad Nacional de La Plata, 1900 La Plata, Argentina.*
*megus@quimica.unlp.edu.ar

Abstract——**In the present work, the heteropolymolybdate $(NH_4)_6MnMo_9O_{32}$ containing Mn(II) as heteroatom was synthesized. The microcrystalline precipitate was characterized by XRD, FTIR, Raman spectroscopy, and SEM-EDS. Although the SEM-EDS results showed a surface enrichment of Mo, the expected structure was verified by FTIR and Raman spectroscopy. According to its chemical and structural properties, the MnMo9 system was evaluated as "bulk" in the clean oxidation of diphenyl sulfide (DPS) and dibenzothiophene (DBT) with H_2O_2 at 80ºC. The results showed high reactivity, with 100% conversion of both DPS and DBT in short reaction times and good selectivity to the corresponding sulfones. Compared to other HPOMs, this species showed higher activity and selectivity to sulfone in DBT.**

Keywords—— *heteropolymolybdates, selective oxidation, diphenyl sulfide, dibenzothiophene, hydrogen peroxide*

I. INTRODUCTION

The intensive use of fossil fuels containing sulfur causes serious environmental problems, such as fog and acid rain. In the last decade, the exhaustive desulfurization of fossil fuels to obtain ultra-low sulfur diesel for transportation has attracted worldwide attention due to increasingly strict environmental regulations and the consequences that the presence of pollutants generates for the environment (acid rains, global warming). Currently, hydrodesulfurization (HDS) is the main desulfurization method in the oil processing industry, but HDS requires aggressive environmental conditions that involve high operating costs. Also, HDS is not efficient in the conversion of some refractory sulfides. As a result, researchers have been working to develop low-cost alternative or complementary technologies to HDS. Alternative desulfurization technologies have been developed in recent years, including oxidative desulfurization (ODS), extractive desulfurization (EDS), adsorption desulfurization, etc. Among these technologies, oxidative desulfurization (ODS) is proposed as one of the most effective methods due to its mild operating conditions, low cost, and excellent ability to remove aromatic thiophenic compounds. In the ODS process, organic sulfides are oxidized to sulfones, which can be easily removed by simple physicochemical operations such as extraction or adsorption. The use of appropriate oxidants is a priority factor in both cost and environmental aspects. Hydrogen peroxide (H_2O_2) is considered a promising oxidant due to its high reactivity and the low environmental impact generated by its products; the reaction produces only H_2O, it is relatively cheap, it does not generate polluting residues, and it is safe (Campos-Martin *et al*., 2010; Egusquiza *et al*., 2021; Houda *et al*., 2018; Ismagilov *et al*., 2011; Li *et al*., 2020; Muñoz *et al*., 2014; Muñoz *et al.,* 2017; Puello Polo *et al*., 2014; Sato *et al.*, 2001; Srivastava, 2012; Zapata *et al.*, 2005)

Molybdenum and/or tungsten iso/heteropolyanions are of interest in various fields of chemistry due to their high reactivity and structural versatility. For this reason, these systems find various applications in catalysis, medicine, and other fields such as inorganic chemistry. Structurally, the systems share MO_6 octahedrons (M= W and/or Mo), which can also join a third ion or "heteroatom" in tetrahedral or octahedral coordination, for example, P(V), Co(II), Ni(II), Fe(II)/(III), V(V)/(IV), etc. Depending on the type of heteroatom and the possibilities of bonding to the MO_6 octahedrons, there is a great variety of heteropolyanions with different polymeric structures. The two best known groups are those based on Keggin, $H_nXM_{12}O_{40}$, and Dawson, $H_nX_2M_{18}O_6$, structures (Pope,1983; Pope and Müller, 1991; 1994).

In the present work, the heteropolymolybdate of formula $(NH_4)_6MnMo_9O_{32}$ (Waugh phase, MnMo9) (Botto, *et al.,* 1992; Zammel, *et al.,* 2015) was synthesized and characterized. Given the chemical and structural properties of this phase, its catalytic behavior in the clean oxidation of diphenyl sulfide (DPS) and dibenzothiophene (DBT) was analyzed.

II. METHODS

A. Synthesis and characterization

The heteropolymolybdate containing Mn(IV) as heteroatom was obtained by crystallization from Mn/Mo aqueous solutions in stoichiometric proportions (Mn:9Mo) prepared by the oxidation of Mn(II) with H_2O_2 in NH_4OH media, and $(NH_4)_6Mo_7O_{24}$. The deep yellow solid obtained was separated from the solution by filtration and allowed to dry in air at room temperature.
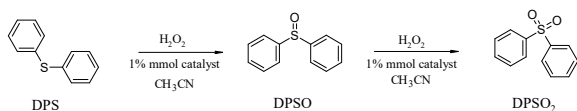
Scheme 1: Selective catalytic oxidation of DPS in the presence of H_2O_2.

Scheme 2: Selective catalytic oxidation of DBT in the presence of H_2O_2.

Characterization was performed by X-ray powder diffraction (XRD) using a Philips X'Pert (graphite monochromator) operating at 40 kV and 45 mA (Ni filter, Cu Kα radiation λ= 0.1542 nm); SEM-EDS microscopy in a Philips 505 microscope equipped with EDAX 9100 microprobe; vibrational infrared spectroscopy (FTIR) with Bruker IFS 66 FTIR equipment using KBr pellets and Raman microprobe in a Via Renishaw spectrometer equipped with a CCD detector and integrated with a Leica DLML confocal optical microscope, Ar$^+$ laser line of 488 nm and resolution of 2 cm^{-1}.

The reduction studies were carried out by the temperature-programmed reduction (TPR) technique, and the reactor was fed with a 10% H_2 reducing agent in an N_2 stream, from 20 to 875°C at a heating rate of 10°C min^{-1}. The hydrogen consumed was detected by a thermal conductivity cell.

B. Catalytic evaluation
The oxidation reaction was carried out in batch at acetonitrile reflux, using 1% mmol of catalyst, H_2O_2 as excess oxidant, and 1 mmol (5.3×10^3 ppm S) of DPS or DBT (substrate/oxidant ratio, 1/20).

Aliquots were taken at different time intervals. The catalyst was evaluated in the selective oxidation of DPS or DBT (substrate/oxidant ratio, 1/20) to the corresponding sulfoxide (DPSO/DBTO) and/or sulfone (DPSO$_2$/ DBTO$_2$) using H_2O_2 as clean oxidant (Scheme 1 and 2 respectively). The reaction was carried out in batch, with 0.01 mmol of catalyst, under stirring at reflux of acetonitrile, in excess of oxidant (H_2O_2 35%, 1 mL). The advance of the reaction was followed by thin-layer chromatography (TLC), and quantification was performed by gas chromatography (GC) in a Shimadzu 2014 chromatograph equipped with a 30 m × 0.32 mm SPB-1 capillary column and FID detector. The composition was determined by the area normalization method. These reactions are represented in Schemes 1 and 2.

The turnover number (TON) was calculated by dividing the number of molecules obtained by the number of catalyst molecules used in the reaction. And we calculated turnover frequencies (TOF) by dividing the number of molecules of product obtained by the number of catalyst molecules used in the reaction in time unit (min),

$$TON = \frac{n_{product} \times X}{n_{catalyst}} \qquad (1)$$

$$TOF(min^{-1}) = \frac{\frac{n_{product} \times X}{n_{catalyst}}}{time} \qquad (2)$$

Table 1. Semiquantitative chemical analysis data and SEM-EDS spectrum of $(NH_4)_6MnMo_9O_{32}$. Values expressed in (%) by weight and in (%) atoms of element.

Mo/Mn	Theor.	Exp.
Wt (%)	15.72	33.96
At (%)	9.00	19.49

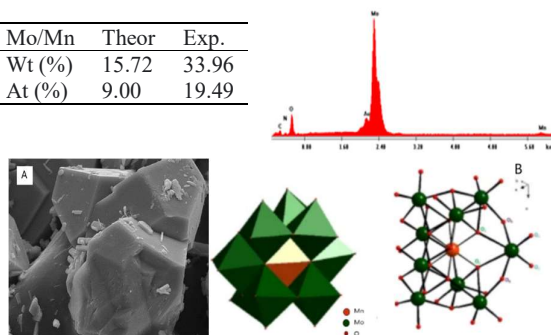Figure 1: A) SEM microphotograph and B) structural representation of the Waugh-type phase, $(NH_4)_6MnMo_9O_{32}$

Figure 2: XRD of $(NH_4)_6MnMo_9O_{32}$

where n product is the mmols of product obtained at 30 min of reaction, n catalyst is the mmols of catalyst, X is the conversion at 30 min of reaction, and time is reaction time.

III. RESULTS
A. Synthesis and characterization
The microcrystalline precipitate obtained was characterized by semiquantitative EDS analysis, SEM, XRD, vibrational FTIR, and Raman spectroscopy.

The semiquantitative chemical composition data obtained by SEM-EDS show an increase of both elements on the surface of the crystals, with a preponderance of Mo over Mn, Table 1. This effect is probably due to the presence of surface Mo(IV) oxides.

Sometimes a partial reduction of Mo at the synthesis temperature in the presence of NH_4^+ can occur, so MoO_x oxide appears in a small proportion.

The XRD pattern is presented in Fig. 2. By comparison with the literature, the presence of the HPOM, Waugh type, was verified as the majority phase (PDF 851653, red lines in the Fig. 1). The presence of MoOx (PDF010706, #), Mn oxides in different oxidation states (PDF 652776, *) and Mn and Mo mixed oxides (PDF 842102, +) can also be observed. The peaks at 2θ =

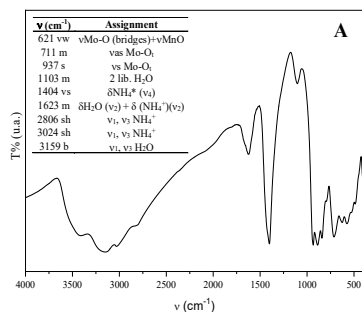29.9 and 30.3 are due to the presence of MnMoO$_4$ (PDF 780221, &).

ν (cm^{-1})	Assignment
621 vw	νMo-O (bridges)+νMnO
711 m	νas Mo-O$_t$
937 s	νs Mo-O$_t$
1103 m	2 lib. H$_2$O
1404 vs	δNH$_4$* (ν$_4$)
1623 m	δH$_2$O (ν$_2$) + δ (NH$_4^+$)(ν$_2$)
2806 sh	ν$_1$, ν$_3$ NH$_4^+$
3024 sh	ν$_1$, ν$_3$ NH$_4^+$
3159 b	ν$_1$, ν$_3$ H$_2$O

Figure 3: (A) FTIR spectra and (B) Raman microanalysis of the (NH$_4$)$_6$MnMo$_9$O$_{32}$ phase according to Botto *et al.* (1992).

The Waugh structure (1:9) is composed of nine condensed MoO$_6$ octahedrons that share oxygen atoms forming the anionic framework of the complex [MnMo$_9$O$_{32}$]$_6^-$ The Mn(IV) atom located in the center of the anion is coordinated by six bridging oxygen atoms bonded to Mo atoms (Lin *et al*., 2000). As proposed by Pope (1983) and Pope and Müller (1991), it can also be described as a "derivative" of the Keggin type [XM$_{12}$O$_{38}$], as seen in Fig. 1 B), where two sets of three octahedra were removed, leaving "gaps" or vacancies at the vertices of an equilateral triangle. In this way two isomeric structures (L- and D-) of [MnMo$_9$O$_{32}$]$^{6-}$ (Zammel *et al*., 2015) could be obtained.

For the vibrational analysis, it is convenient to consider the different types of Mo–O bonds in the vibrational study of the heteropolymetalate (Botto *et al*., 1992). According to the structure, three types of Mo–O bonds can be clearly distinguished in the [MnMo$_9$O$_{32}$]$^{-6}$ framework: Mo–O$_t$ terminal groups (Mo–O$_t$); Mo-O-Mo bridge bonds involving Mo atoms located in the self-plane (top or bottom) or different planes (top-middle, bottom-middle); Mo–O–Mn bonds. The infrared and Raman spectra are shown in Fig. 3(A and B); in the FTIR spectrum the bands corresponding to the Mo–O modes are not particularly evident. The intense band (Fig. 3A) at 1404 cm^{-1} together with the bands at 2806 and 3024 cm^{-1} correspond to the deformations of NH$_4^+$ (Botto *et al.,* 1992; Zammel *et al.,* 2015; Lin *et al*., 2000); and the band at 1623 cm^{-1} corresponds to the vibrational modes of H$_2$O.

The Raman spectrum is presented in Fig. 3B. The lines found in the 1000-600 cm^{-1} region can be attributed to Mo–O stretching modes of different structural complexity, while those found at lower wavenumbers (400-200 cm^{-1}) are assigned to bending and strain modes (Fournier *et al.,* 1991; Hardcastle and Wachs*,* 1990; Mestl and Srinivasan*,* 1998; Tian *et al.,* 2010; Williams *et al.,* 1991). In Fig. 3, the intense Raman lines at ~946 and 919 cm^{-1} correspond to the symmetric and antisymmetric Mo–O$_t$ deformations of the MoO$_6$ units. The group of lines of weak intensity in the 885-800 cm^{-1}

zone can be attributed to the antisymmetric stretching modes, and those of low intensity at ~568, 638 and 703 cm^{-1} are associated with the antisymmetric and symmetric vibrations, respectively, of the Mo–O–Mo/Mn bridging bonds
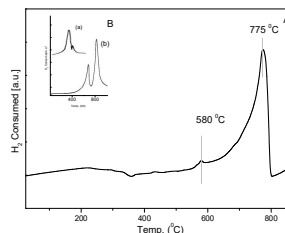

Figure 4: A) TPR patterns of (NH$_4$)$_6$MnMo$_9$O$_{32}$; B) comparative patterns of a) MnO$_2$, b) ammonium heptamolybdate.

characteristic of HPOMs (Camacho-Lopez *et al.,* 2011; Mestl and Srinivasan*,* 1998; Tian *et al.,* 2010).

Temperature-programmed reduction technique constitutes a useful tool in the study of catalysts, since it allows analyzing the redox behavior of the individual metallic species in the polymetallic matrix. In the present work TPR provides information about the redox behaviour of the Mo(VI) and Mn(IV) species present in the heteropoly compound. It is well known that the results are usually due to external factors such as the crystal size, heating rate, etc. (Jones and McNicol, 1986). The TPR pattern of (NH$_4$)$_6$[MnMo$_9$O$_{32}$].8H$_2$O is shown in Fig. 4, where the TPR patterns of ammonium heptamolybdate and MnO$_2$ are embedded for comparative purposes. The ammonium heptamolybdate shows two peaks at 721 and 843 °C corresponding to the formation of MoO$_2$ and metallic molybdenum, while MnO$_2$ presents signals at 370 and 398 °C attributable to successive reductions to Mn(III) and Mn(II) (Botto *et al.,* 1992). The reduction of the Waugh phase was performed. In our working conditions, two reduction steps are clearly observed in Fig. 4 at 580 and 775 °C (and incipient signal at 875 °C, the maximum temperature that can be reached under the experimental conditions), which can be attributed to the reduction of Mo due to its greater proportion in the HPOMs. Also, very weak additional lines could be observed at 330, 376, 440 °C.

The sequence proposal slightly shifted at higher temperatures according to the bibliography (Botto *et al.,* 1992), for the Mo reduction species is:

$$Mo(VI) \text{ (from MnMo}_9) \xrightarrow{440°C} MoO_3 \xrightarrow{580°C} Mo_4O_{11} \xrightarrow{775°C} MoO_2.$$
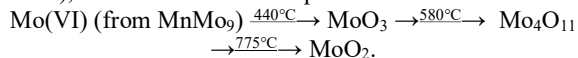
Due to the small Mn content in the lattice, the lines corresponding to the manganese compounds are very weak (Botto *et al.,* 1992). Therefore, the following sequence for Mn(IV) can be suggested:

$$Mn(IV) \text{ (from MnMo9)} \rightarrow \xrightarrow{330°C} Mn(III) \rightarrow \xrightarrow{580°C} Mn(II)$$
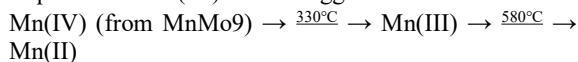
The shift to higher reduction temperatures would be related to the incorporation of manganese ions in some

oxidic systems (Cordischi *et al.*, 1987). In fact, the Mn(II) is expected to be incorporated into the MoO_2 lattice, forming a mixed oxide. Finally, the last step in the reduction of molybdenum leads to the formation of metallic Mo phase (not presented in Fig. 4).

As we have shown in previous works on HPOMs based on Anderson XMo_6 phases (with X=Co, Ni, Cr, Rh, etc.), the X-Mo interaction causes an increase in the reducibility and reactivity of Mo, giving rise to a synergistic effect during catalysis. (note that the Mo reduction T decreases about 75°C in $MnMo_9$ with respect to Mo in HMA). This type of interaction and increase in X-Mo reactivity has also been observed in thermal treatments in an oxidizing or inert atmosphere using TG-DTA. In the present work it is shown that Mn also induces Mo reducibility (Cabello *et al.*, 1994; Cabello *et al.*, 2006; Jones and McNicol, 1986).

B. Catalytic evaluation

According to the redox properties of this phase, it was analyzed as a catalyst in the clean oxidation of diphenyl sulfide and dibenzothiophene. The reaction was carried out in batch with stirring at 800 rpm, to minimize mass transfer limitations (Egusquiza *et al.*, 2021).

In the absence of a catalyst, this reaction occurs with very low yield (8% in 10 h) in excess of H_2O_2.

Furthermore, considering that HPOMs have a comparatively low surface area, the catalytic process occurs on the external surface of the solid, and the low surface tension acetonitrile used as solvent facilitates mass transfer.

Figure 5 shows the high reactivity, with 100% conversion of both DPS and DBT in less than 20 min of reaction.

For both reactions, the catalyst was selective for the corresponding sulfone (TON/TOF in Table 2), detecting only DBT sulfoxide (DBTO) at the beginning of the reaction, which is quickly converted to DBT sulfone ($DBTO_2$).

The catalytic behavior could be compared with that obtained previously for Anderson phases of the general formula $[Ni(II)(Mo/W)(VI)_6O_{24}H_6]^{4-}$ ($NiMo_6$) because the HPOM size is similar to that of $MnMo_9$, and DPS reaction conditions were similar. Studies on $NiMo_6$ revealed that the Ni-Mo system was only selective for sulfoxide production (76% selectivity) with 90% conversion, given a higher TON/TOF for DPSO, as shown in Table 2.

The system $MnMo_9$ was also compared with another system containing Mn, the derived Keggin type sandwich phase called PWMn of general formula $[Mn_4(H_2O)_2(PW_9O_{34})_2]^{10-}$ (Egusquiza *et al.*, 2021). The PWMn system in excess of oxidant presented higher selectivity to DPSO (Table 2, higher TON/TOF for sulfoxide), but the $MnMo_9$ system was selective to the respective sulfone.
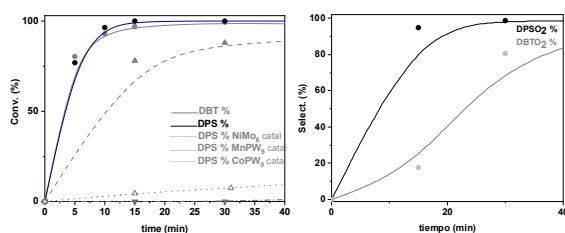
Figure 5: Conversion for DBT and DPS as a function of time catalyzed by the $(NH_4)_6MnMo_9O_{32}$ phase.

Table 2. Comparison of the effect of catalyst (TON and TOF) for corresponding sulfoxide and/or sulfone synthesis.

Catalyst	Substrate	Sulfoxide		Sulfone	
		TON	TOF $(x10^{-2})$	TON	TOF $(x10^{-2})$
$MnMo_9$	DPS^	-	-	10.00	33.30
$MnMo_9$	DBT^	0.10	0.33	9.80	32.67
$NiMo_6$	DPS^	5.90	19.67	1.90	6.33
PWMn	DPS*	0.17	0.57	-	-
PWMn	DBT*	0.03	0.10	-	-
PWCo	DPS*	0.54	1.80	2.70	0.09

^ H_2O_2; * t-BuOOH

The comparison of results with that previously obtained with the PW_9Mn phase suggests that the activity is related with the presence of the metal. In this sense, the redox character of metallic species, the stability of its oxidation state, the chemical affinity toward the reactive and the M local symmetry play an important role to definite the following activity order $MnMo_9 > NiMo_6 > PWCo > PWMn$. Mn presents higher oxidation states while Co(II)-Co(III) oxidation is relatively difficult in absence of adequate environment. The better activity in the $MnMo_9$ system can be associated with the redox activity of Mn and synergic effect that generates the presence the Mn in the Mo matrix to favor the catalytic activity.

A plausible mechanism of the ODS reaction involves the formation of peroxo-molybdate species and the subsequent nucleophilic attack of the sulfur atom in the sulfide on the peroxo species. Indeed, it is known that thioethers are oxidized to sulfoxides by electrophilic oxidants. Mechanistically, it is believed that the electrophilicity of the peroxide oxygen of H_2O_2 is increased by an oxometal group ($Mo=O_d$) in the HPOM. As far as H_2O_2 decomposition is concerned, thermal decomposition of H_2O_2 to singlet oxygen $^1O_2$ in water is significant in basic aqueous solution at temperatures above 323K. Taking into account that the H_2O-H_2O_2 system has a pH < 7 at any H_2O_2 concentration, the decomposition process can be disregarded in our experimental conditions. (Maciuca *et al.*, 2008)

IV. CONCLUSIONS

It was possible to synthesize and characterize the $(NH_4)_6MnMo_9O_{32}$ phase.

Given its chemical and structural properties, its catalytic activity in the clean oxidation of DPS and DBT was evaluated. A 100% conversion of both reagents was achieved in less than 20 min of reaction, with good selectivity to the corresponding sulfone.

Compared to other Anderson or Keggin derived HPOMs, the $MnMo_9$ is the most reactive because Mn

4

presence, which produces a higher oxidation of sulfide to give the respective sulfone, considering the electron mobility in the redox processes.

It is interesting to note that the $MnMo_9$ phase as a bulk catalyst achieved the oxidation of DBT, a reagent that is difficult to oxidize with other HPOM-based catalysts due to steric factors.

Due to the promising results obtained, we will carry out the study of the supported catalyst in different synthetic and natural oxidic systems.

ACKNOWLEDGEMENTS

REFERENCES

Botto, I.L.; Cabello, C.I. and Thomas H.J. (1992) Thermal behaviour and properties of the $(NH_4)_6MnMo_9O_{32}·8H_2O$ Waugh phase. *Thermochimica Acta.* **211**, 229-240.

Cabello, C.I.; Botto, I.L. and Thomas H.J. (1994) Reducibility and Thermal Behaviour of some Anderson Phases. *Thermochimica Acta.* **232**, 183.

Cabello, C.I.; Munoz, M.; Botto, I.L. and Payen E. (2006) The role of Rh on a substituted Al-Anderson heteropolymolybdate: Thermal and hydrotreating catalytic behavior. *Thermochimica Acta.* **447**, 22-29.

Camacho-López, M.A., Escobar-Alarcón, L., Picquart, M., Arroyo, R., Córdoba, G. and Haro-Poniatowski, E. (2011) Micro-Raman study of the m-MoO_2 to α-MoO_3 transformation induced by cw-laser irradiation. *Opt. Mat.* **33**, 480-484.

Campos-Martin, J.M., Capel-Sanchez, M.C., Perez-Presas, P. and Fierro, J.L.G. (2010) Oxidative processes of desulfurization of liquid fuels. *J. Chem. Technol. Biotechnol.* **85**, 879-890

Cordischi, D., Gazzoli, D., Valigi M. and Botto, I.L. (1987) Incorporation of manganese ions in magnesium titanate: A structural thermogravimetric, optical (reflectance) and electron spin resonance study. *React. Solids.* **4**, 125

Egusquiza, M.G., Soriano, M.D., Muñoz, M., Romanelli, G., Soriano, J., Cabello, C.I. and López Nieto, J.M. (2021) Precursors of tetragonal tungsten bronzes as catalysts in selective reactions: Liquid phase oxidation of diphenyl sulfide and gas phase oxidation of hydrogen sulfide. *Cat. Tod.* **372**, 70-81.

Fournier, M., Thouvenot, R. and Rocchiccioli-Deltcheff, C. (1991) 31P NMR MAS Spin-lattice relaxation as a dispersion probe: an easy access to active-site concentration in silica-supported dodecamolybdophosphoric acid. *J. Chem. Soc., Faraday Trans.* **87**, 349-351.

Hardcastle, F.D. and Wachs, I.E. (1990) Determination of molybdenum–oxygen bond distances and bond orders by Raman spectroscopy. *J. Raman Spectrosc.* **21**, 683-691.

Houda, S., Lancelot, C., Blanchard, P., Poinel, L. and Lamonier. C. (2018) Oxidative Desulfurization of Heavy Oils with High Sulfur Content: A Review. *Catalysts.* **8**, 344.

Ismagilov, Z., Yashnik, S., Kerzhentsev, M. Parmon, V., Bourane, A., Al-Shahrani, F.M., Hajji, A.A. and Koseoglu, O.R. (2011) Oxidative Desulfurization of Hydrocarbon Fuels. *Cat. Rev.-Sci. Eng.* **53**, 199-255.

Jones, A. and McNicol, B. (1986) *Temperature-programmed Reduction for Solid Materials Characterization*, Marcel Dekker Inc., New York

Li, J., Yanga, Z., Hub, G. and Zhao J. (2020) Heteropolyacid supported MOF fibers for oxidative desulfurization of fuel. *Chem. Eng. J.* **388**, 124325.

Lin, S., Zhen, Y., Wang, S. and Dai Y. (2000) Catalytic activity of $K_{0.5}(NH_4)_{5.5}[MnMo_9O_{32}]·6H_2O$ in phenol hydroxylation with hydrogen peroxide *J. Mol. Catal. A: Chemical.* **156**, 113-120.

Maciuca, A.L., Ciocan, C.E., Dumitriu, E., Fajula, F. and Hulea V. (2008) V, Mo and W-Containing Layered Double Hydroxides as Effective Catalysts for Mild Oxidation of Thioethers and Thiophenes with H_2O_2. *Catal. Today.* **138**, 33-37.

Mestl, G.T. and Srinivasan, K.K. (1998) Raman Spectroscopy of Monolayer-Type Catalysts: Supported Molybdenum Oxides *Catal. Rev. Sci. Eng.* **40**, 451-570.

Muñoz, M., Egusquiza, M.G., Botto, I.L. and Cabello. C.I. (2014) Structural and Compositional Effect of Heteropolyoxoanions $[NiMo_{6-x}W_xO_{24}H_6]^{-4}$ on the Catalytic Activity of Clean Selective Oxidation of Diphenylsulfide. *Current Catal.* **3**, 139-146.

Muñoz, M., Gallo, M.A., Gutiérrez-Alejandre, A., Gazzoli, D. and Cabello, C.I. (2017) Molybdenum-containing systems based on natural kaolinite as catalysts for selective oxidation of aromatic sulfides. *Appl. Catal. B: Environ.* **219**, 683–692.

Pope M.T. (1983a) *Heteropoly and Isopoly Oxometalates*. Springer-Verlag, Berlin.

Pope, M.T. and Müller A. (1991b) Polyoxometalate chemistry: an old field with new dimensions in several disciplines. *Angew. Chem. Int. Ed. Engl.* **30**, 34-48.

Pope, M.T. and Müller A. (1994c) *Polyoxometalates from Platonic Solids to Antiviral Activity*, Kluwer, Nether.

Puello Polo, E., Cabello, C.I. and Gazzoli, D. (2014) $MoOx-ZrO_2$ System: Preparation, Characterization and Catalytic Activity for Selective Oxidation of Diphenylsulfide. *Current Catalysis* **3**, 172-178.

Sato, K., Hyodo, M., Aoki, M., Qi Zheng, X. and Noyori, R. (2001) Oxidation of sulfides to sulfoxides and sulfones with 30% hydrogen peroxide under organic solvent-and halogen-free conditions. *Tetrahedron.* **57**, 2469-2476.

Srivastava, V.C. (2012) An evaluation of desulfurization technologies for sulfur removal from liquid fuels. *RSC Advances.* **2**, 759-783.

Tian, H., Roberts, C.A. and Wachs, I.E. (2010) Molecular Structural Determination of Molybdena in Different Environments: Aqueous Solutions, Bulk Mixed Oxides, and Supported MoO_3 Catalysts. *J. Phys. Chem. C* **114**, 14110-14120.

Williams, C.C., Ekerdt, J.G., Jehng, J.M., Hardcastle, F.D. and Wachs, I.E. (1991) A Raman and ultraviolet diffuse reflectance spectroscopic investigation of silica-supported molybdenum oxide. *J. Phys. Chem*. **95**, 8781-8791.

Zammel, D.; Nagazi, I. and Haddad A. (2015) Synthesis and Characterization of a Novel Waugh-Type Polyoxometalate $K_{1.5}(NH_4)_{4.5}[MnMo_9O_{32}]4.2H_2O$. *J. Clust. Sci*. **26**, 1693-1706.

Zapata, B., Pedraza, F. and Valenzuela, M.A.; (2005) Catalyst screening for oxidative desulfurization using hydrogen peroxide. *Catal. Today*. **106**, 219-221.